ELSEVIER

Journal of Power Sources 86 (2000) 369–375

JOURNAL OF POWER SOURCES

www.elsevier.com/locate/jpowsour

Integrated fuel cell system with tubular solid oxide fuel cells

R.J. Boersma *, N.M. Sammes, C. Fee

The Department of Materials and Process Engineering, The University of Waikato, Private Bag 3105, Hamilton, New Zealand

Accepted 5 October 1999

Abstract

An integrated fuel cell system based on tubular fuel cells is examined. The system relies on free convection to pass air and spent gas through the system by using a chimney. Thus, an expensive air supply mechanism is not required. It is shown that the use of free convection up to a power generating scale of around 2 kW is feasible. Factors determining the dimensions of the heat exchanging system are studied. A complete system capable of generating 2 kW of electricity, running on natural gas and ambient air, is anticipated to have a diameter of approximately 300 mm and a height of 1700 mm. Including the chimney a total height of 5 m was found.

Keywords: Solid oxide fuel cell; System modelling; Tubular

1. Introduction

With fuel cell materials and stacks nearing commercialisation there is an increasing need for low cost systems that can sustain the process conditions required for fuel cell operation.

System studies have demonstrated that the balance of plant of a fuel cell system may cost substantially more than the fuel cell itself. This is especially so for smaller systems, which in recent years have become the subject of extensive research and development. Cost targets of 1000 US$/kW have frequently been stated as targets for the commercial uptake of fuel cells. This is unlikely to be different for small systems, since these will in many applications have to compete with electricity supply systems that are already competitive at this cost level.

Here, an SOFC system outlined which consists of a number of concentrical tubes, which are used for exchanging heat from exiting gases with incoming gases. A similar system has been described by Möbius [1]. The process air and spent gases are drawn through the system using a chimney. The SOFC being considered in this study consists of tubular cells, which are mounted vertically on a base plate. Control of the air temperature takes place by installing a flow restriction in the chimney, the position of which is controlled by a thermocouple located near the fuel cells. The principles discussed herein have been studied extensively by means of modelling calculations, for an array of tubular fuel cells. The principles possibly also apply to a planar system.

The simplicity and robustness of the balance of plant leads to a cheap system which can be made to operate reliably at an affordable cost.

2. System description

The system being studied in this paper is shown in Fig. 1. An array of SOFC tubular cells is mounted on a metallic base plate. A glass ceramic seal secures the tube to the base plate and ensures that the fuel flows only through the inside of the tube [2,3]. Air passes around the outside of the tubes and provides the oxygen. At the end of the tubes the spent fuel mixes with the spent air and combusts, raising the temperature to well over 1000°C. The spent gas is forced downwards to exchange heat with the incoming air, which passes through a tube placed inside the tube through which the spent gas passes. The hot air in turn heats the fuel to the required inlet temperature by placing a tube inside the air tube.

After exchanging part of its heat, the combusted gas flows radially outward and upward to a chimney, which creates the draft for the gases to pass through the system at the required flow. While flowing radially outward and upward the combusted gas exchanges heat with the incom-

* Corresponding author

0378-7753/00/$ - see front matter
PII: S0378-7753(99)00410-3

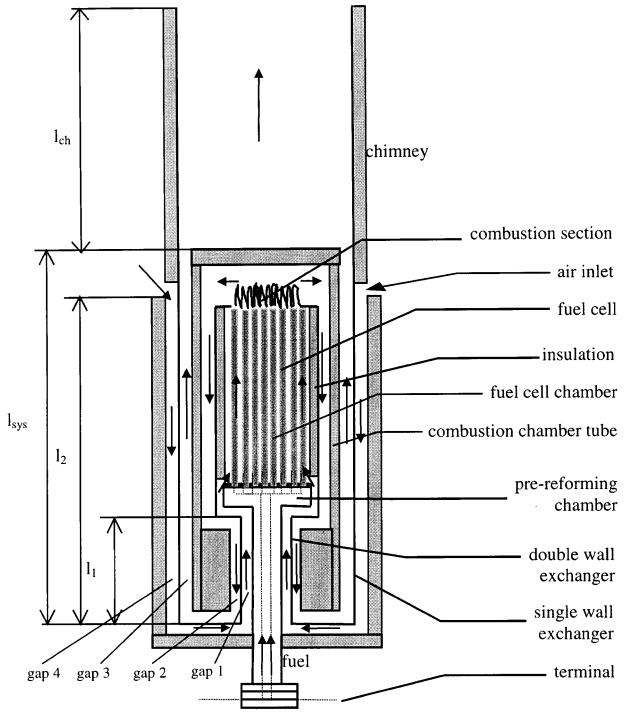

Fig. 1. Schematic drawing of the system.

ing air through a circular plate at the bottom of the system and then through a tube placed around the system. Thus, air is heated firstly through a single wall heat exchanger and then through a double wall heat exchanger. In the double wall heat exchanger the air gives up part of its heat to the fuel, which is only heated in the double wall exchanger.

Insulation material is applied in the system at appropriate locations. Insulation material is placed around the tube containing the cells, as otherwise the combusted gas would increase the temperature of the cells, which would lead to higher airflows or greater temperature differences along the cells. There is also insulation material around the tube along which the exhaust gas passes downwards and then later upwards. This prevents loss of heat to colder sections before heat can be exchanged with the incoming air and fuel.

To allow operation on natural gas, a pre-reforming catalyst is placed in the space below the cells. A non-soot forming mixture of natural gas and steam has to be supplied.

The cells of the system are currently under development. These will consist of an anode-supported tube, while the electrolyte consists of a thin layer of 8YSZ, with a thickness of approximately 20 μm. Because the electrical current has to be transported to the base plate along the electrodes, the resulting electrical losses can become excessive if cells are made too long. It was found in previous work that if lengths of up to 100 mm are used, losses will be within 10% of the electrical power produced at the electrodes of the cell [4]. Longer cells can be made by joining cells and connecting them electrically in series.

Mass and heat transfer effects of the system are examined at various conditions and heat exchanger performance optimised by varying the gaps between the heat exchanger tubes, with the constraint that the system, including its chimney, should not become excessively long. Thus, an optimum of minimum friction to flow and maximum heat transfer is found.

3. The model

3.1. Input parameters

The model used to simulate the system is described in Ref. [5]. The modelling equations were programmed in a Mathcad file, which consists of three main modules. The first is an input–output module. The second module calcu-

Table 1
Independent variables used in this study

Description	Symbol	Range	Remark
Fuel inlet temperature	T_{f1}	248–298 K	
Air inlet temperature	T_{c2}	248–298 K	
Fuel utilisation	x_f	0.7	Not varied
Cell voltage	V	0.6–0.85 V	
Double wall heat exchanger length	l_1	0.2–2 m	Can be replaced by T_{c0} and T_{f0}, being the temperatures at which oxidant and fuel enter the cells
Single wall heat exchanger length	l_2	0.2–2 m	
Inner diameter fuel supply tube	D_{1i}	16–120 mm	Depending on rated power of system
Number of cells	n_{cell}	60–154	Determines power rating of the system
Cell length	l_c	100–200 mm	
Gap for air flowing upward in d.w. section	gap1	0.005–0.02 mm	
Gap for exhaust gas, flowing downward in d.w section	gap2	0.005–0.02 mm	
Gap for exhaust gas moving upward in s.w. section	gap3	0.005–0.02 mm	
Gap for air flowing downward in s.w. section	gap4	0.005–0.02 mm	
Wall thickness of tubes	t	1 mm	Not varied

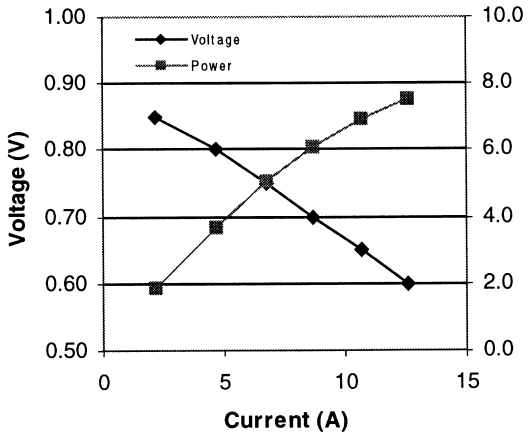

Fig. 2. *I–V* characteristic of a 100 mm long tubular SOFC, according to the model presented in [2]. The cell runs on dry hydrogen at a hydrogen utilisation of 70%.

lates the mass and energy balance of the cells, the burner and the two heat exchangers together and verifies the overall energy balance. The energy balance of the single wall and double wall heat exchanger are modelled in the third module which calculates the respective energy balances and dimensions these using semi-empirical relations for calculating heat transfer coefficients [6]. Average heat transfer coefficients are calculated at each wall in dependency of the average temperature of the flow media. The physical properties such as viscosity, heat conductivity, Prandtl number etc. are calculated in dependency of the average temperature using well established relations for viscosity and conductivity of the gases containing a single species, and a mixtures of gases, as described in [7].

Table 1 lists the set of independent variables used in this study. Since cell voltage, cell current and fuel utilisation are related, only two need to be specified. In this study the cell current was treated as the dependent variable, and could therefore be left out from the table. The relation for a cell running on hydrogen with 2% water and constant utilisation of 70% is shown in Fig. 2. The *I–V* characteristic was found using the model described in Ref. [4].

Table 2
Systems studied in this paper. The cells can actually be placed on a base plate 10 mm smaller than the stated values. The plates were made somewhat larger for manufacturing reasons

Number of cells	Diameter base plate (mm)	Cell length (mm)	Rated power
60	106	10	360 W
75	120	20	1 kW
154	170	20	2 kW

The number of cells and the cell diameter determines the diameter of the base plate, which the cells are mounted on (Fig. 3). Table 1 only specifies the number of cells. As will be shown below, there is an optimum for the cell diameter, therefore at that diameter the number of cells only determines the diameter of the base plate. With the holes drilled in the base plate concentrically, the cell area can be plotted vs. the cell diameter. This is shown in Fig. 2 for a cell length of 100 mm. The optimum cell diameter that is found is 6 mm. For the three different systems that were studied, the cell numbers and associated base plate diameter are listed in Table 2.

According to Table 2 the lengths of the heat exchangers can also be varied freely, although not every combination will give rise to favourable process conditions for the fuel

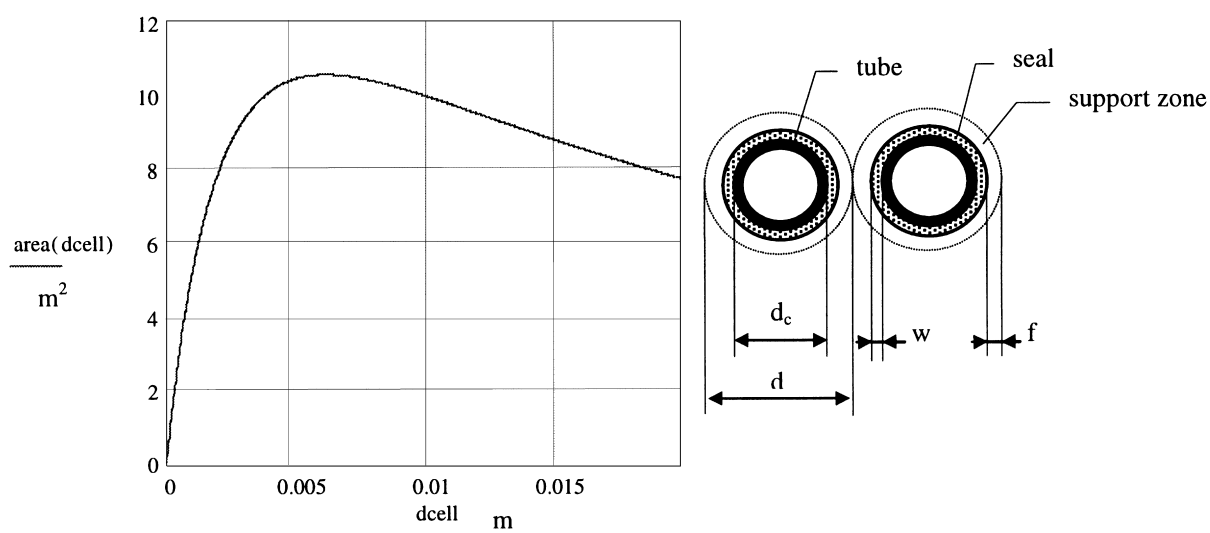

Fig. 3. Cell area (per metre of base plate diameter) as a function of cell diameter for a seal diameter that is 4 mm larger than the cell diameter, and a minimum distance of 2 mm between holes. and thus the diameter of the glass seal is 10 mm. The highest area is found for a cell diameter of 6 mm, therefore the diameter of the holes where the glass seal has to fit in is 10 mm. Holes are assumed to be drilled concentrically, starting in the centre of the base plate.

cells. Instead of using given lengths, they can also be calculated by specifying the fuel and oxidant inlet temperatures. This proved to be a useful method to find an initial set of lengths for the heat exchangers at a given cell voltage. With the lengths thus determined, temperatures were calculated at a range of voltages. It also proved to be a useful method to calculate the effect of variations of the gap sizes on the length of the heat exchangers, while providing the gases at the same temperature in all cases.

The last degrees of freedom listed in Table 1 are the temperatures of the gases entering the system, which were varied from $-25°$ to $+25°$C with the purpose of assessing the effect on the process conditions for the fuel cells.

3.2. Heat exchanger gap variations

The effect of varying the gaps 1–4 (Table 1) on system length and heat exchanger lengths is shown in Table 3 for a 1 kW system. In the calculations the temperature at the end of the cells, just before the burner, is set to 1173.15 K and at the air inlet is set to 983.15 K. The fuel inlet temperature was set 40 K lower.

Noticeable is that an increase of gap 2, the gap through which the exhaust gas passes in the double wall heat exchanger, reduces the length of the double wall exchanger, at a penalty of a small increase in the single wall exchanger length. It is also noticeable that there is a decrease in friction to flow through the system. Additional calculations showed that a further increase of gap 2 of 5 mm leads to an increase of the double wall exchanger length, making it close to the original length. As a result of the increased gap, the heat transfer coefficient from the exhaust gas to the air drops quite sharply.

Increasing gap 3, the gap through which the exhaust gas passes in the single wall exchanger, does not affect the double wall exchanger, and only slightly increases the single wall exchanger length. Increasing gap 3, however, has the second largest effect on the flow friction force of the system, and thus on the chimney length. An 0.05 mm further increase of gap 3 results in an increased length of the single wall exchanger. In that case, the flow friction force of the system reduces somewhat, but the effect on the reduced friction through gap 3 is largely offset by the increase in length of the flow path.

Finally, the combination of a system with gap 2 and gap 3 increased to 15 mm leads to the most favourable combination. The conclusion is that the hottest gases should have a somewhat larger gap than the colder gases. If the gaps become too large then heat transfer is adversely affected.

The last case in Table 3 shows the effect of a similar approach where the base case starts with gaps of 5 mm. In this case the double wall exchanger is reduced significantly in length, with the penalty of a higher frictional force, which results in a longer chimney. The diameter of the chimney is approximately 200 mm and therefore the length to diameter ratio for this case is preferred to the previous case and was used for further calculations.

3.3. Effect of load on cell inlet and outlet temperatures

In a similar fashion, gap sizes were found for the other systems listed in Table 2. The values are given in Table 4. It is of interest to see how the system with the calculated dimensions behaves under different loads. Table 1 is valid for a cell voltage of 0.7 V and a cell current of 8.7 A (460 mA/cm^2) for a cell of 100 mm. Using the I–V curve of Fig. 2 the cell inlet temperatures can now be calculated at a fixed cell outlet temperature. Fig. 4a shows these temperatures as a function of the power produced by the system.

The cell outlet temperature, just before the burner T_{b0}, has been assigned a value of 1173 K, however, it can also be considered as one degree of freedom. To find a solution, either T_{f0} or T_{c0} would have to be fixed. Fig. 4b shows T_{f0} and T_{b0} as a function of the electrical power output at $T_{c0} = 983.15$ K.

Fig. 4a and b give important clues concerning a possible control strategy for the system. One may wish to maintain a constant inlet temperature, since this would put the least thermal stress on the seal construction. A thermocouple, which measures the temperature at the cell inlet, can, through a controller, set the position of a flow restriction in the chimney to obtain a constant inlet temperature. The strategy of Fig. 4b is then followed. One may find, however, that at high power output the outlet temperature

Table 3
Effect of varying the heat exchanger gaps on various dimensions of the system. In all cases l_1 and l_2 were calculated with the requirement of fuel and oxidant inlet temperatures of 943.15 K and 983.15 K respectively. In case 2 a solution could only be found when the fuel inlet temperature was lowered by 6 K

Case	Gap 1 (mm)	Gap 2 (mm)	Gap 3 (mm)	Gap 4 (mm)	l_1 (mm)	l_2 (mm)	l_{sys} (mm)	l_{ch} (mm)	Friction (N)
1	10	10	10	10	888	1080	1158	560	0.134
2	15	10	10	10	975	1077	1245	532	0.127
3	10	15	10	10	706	1125	976	365	0.097
4	10	10	15	10	888	1185	1158	399	0.116
5	10	10	10	15	888	1388	1158	550	0.132
6	10	15	15	10	706	1242	976	251	0.080
7	5	10	10	5	559	812	829	743	0.178

Table 4
Heat exchanger gap sizes for the various systems

System rating	Gap 1 (mm)	Gap 2 (mm)	Gap 3 (mm)	Gap 4 (mm)
365 W	5	5	5	5
1 kW	5	10	10	5
2 kW	5	10	8	4

becomes too high. By placing a second control thermocouple near the top of the cells, control can be redirected to this thermocouple and the control strategy of Fig. 4a can be followed.

3.4. Effect of environment temperature

Fig. 5 shows the effect of varying cell inlet temperatures at system inlet temperatures that are 50 K lower than in the previous cases. Comparison with Fig. 4a shows that the effect is practically negligible. The system responds by requiring a somewhat lower airflow, as a result of which the inlet temperatures drop by only 20 K at full power. The improved heat exchange due to the lower flow explains why the full impact of lowering the inlet temperature by 50 K is not perceived the cells.

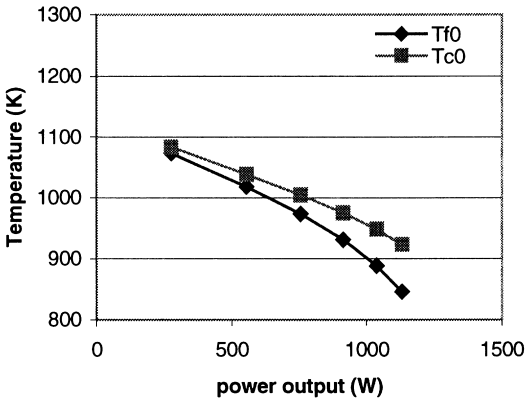

Fig. 5. Cell inlet temperatures at system inlet temperatures of 248 K and a constant cell outlet temperature of 1173.15 K for a 1 kW system.

3.5. Scaling up

When scaling up further, difficulties where encountered with acquiring a fuel inlet temperature that was less than

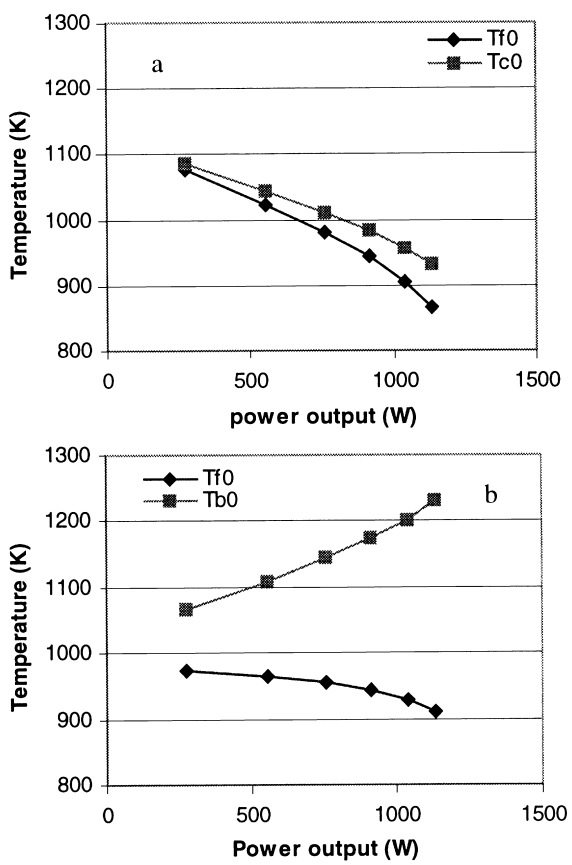

Fig. 4. Effect of electrical power output on fuel and oxidant inlet temperatures at a constant cell outlet temperature of 1173.15 K (a) and effect on fuel inlet temperature and cell outlet temperature at constant oxidant temperature of 983.15 K (b). System inlet temperatures are 298.15 K.

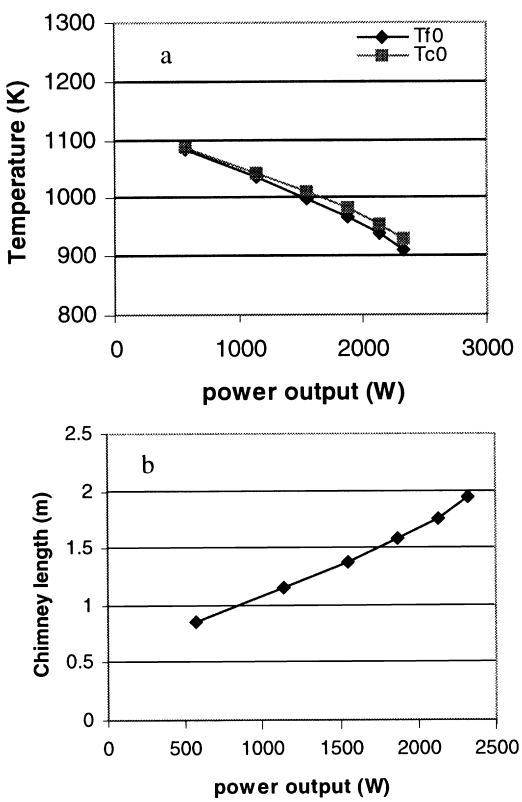

Fig. 6. Cell inlet temperatures for a 2 kW system as a function of electrical power output at a constant cell outlet temperature of 1173.15 K (a), and minimum required chimney length for the different output levels (b).

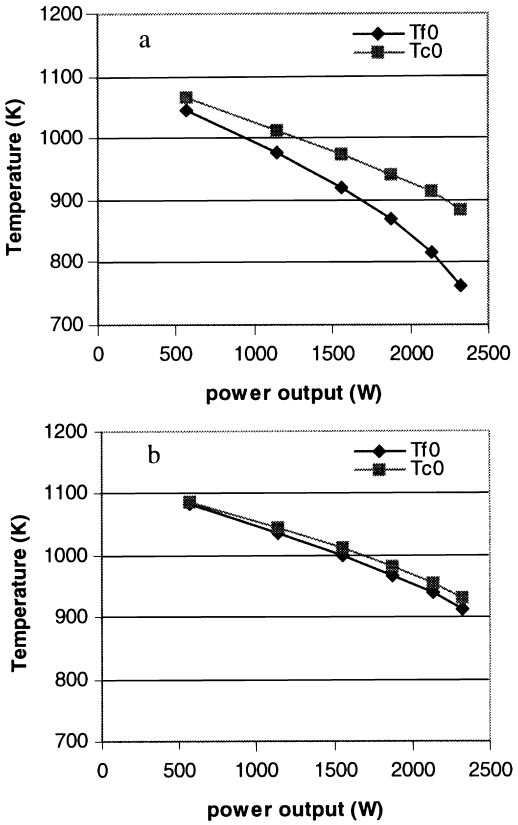

Fig. 7. Cell inlet temperatures for a 2 kW system running on a mixture of methane and steam (1:2). In graph (a) the dimensions are the same as the system of Fig. 6, which runs on dry hydrogen. Because inlet temperatures were considered too, low the single and double wall heat exchanger were both increased in length by 0.7 m. Cell outlet temperatures were kept constant at 1173.15 K.

50 K below the fuel inlet temperature. Increasing the fuel supply tube diameter had a limited effect. It became obvious that heat exchange to the fuel had to be improved. This can be done by inserting a rod with a diameter slightly smaller than the inside of the fuel tube. A rod with a diameter 5 mm smaller than the inner diameter of the fuel tube was used. This improved heat exchange to a satisfactory level. For the 1 kW system, which has a fuel tube inner diameter of 40 mm, the oxidant temperature drops somewhat (2 K), because the fuel becomes hotter. The fuel enters the cells at 15 K below that of the oxidant, which is an improvement compared to the 40 K previously encountered.

For the 2 kW system the inner diameter of the fuel tube was increased to 80 mm and a rod of 70 mm was inserted. This was the maximum fuel tube diameter that could be chosen. The higher this diameter, the shorter the double wall exchanger becomes, as a result of which the single wall exchanger begins to extend to above the combustion chamber. The result is that heat transfer from the spent gas to the air reduces, as heat transfer from the chimney is not as efficient as when gas fills the gap.

Fig. 6 shows the inlet temperatures at a constant outlet temperature of 1173.15 K, along with the minimum chimney length required to draw the gases through the system. In practice a chimney with a fixed length will be used and flow will be controlled by placing a variable flow restriction, for example, a butterfly valve, in either the chimney, or in the air inlet. Control of the setting of the valve can be carried out as discussed before. Fig. 6 demonstrates that, using free convection, a system of 2 kW is feasible, while the system does not need to be excessively large.

To asses the effect of operating the system on natural gas, which is converted partly in the pre-reformer below the cells and partly in the cells, the model had to be extended with a reforming reactor simulator. Because there is no information available on which part of the fuel would be reformed in the pre-reformer, it has been assumed that the entire reforming reaction takes place in the pre-reformer and reaches equilibrium. The heat required for the reaction then causes a temperature drop which follows from $\Delta T = q_r/\mathrm{Cp}$, where q_r is the reforming heat of reaction, which is negative, and Cp is the average heat capacity of the gases entering and leaving the reformer.

So far, little difficulty was encountered when heating the hydrogen to the required inlet temperature. This is because of the high conductivity and low heat capacity of hydrogen. This is different for a mixture of methane and water, which has to be supplied in a mixture of approximately 1 to 2 to prevent the methane from cracking and causing soot formation.

Fig. 7a shows the inlet temperatures at constant cell outlet temperature were the previous 2 kW system to run on a methane water vapour mixture. Unlike the previous cases, here the air enters the double wall exchanger hotter than it leaves it. The heat required to heat the fuel quenches the air. The obvious solution to overcome this problem is to increase the length of the exchangers, which were both increased by 700 mm. At 0.7 V/cell the oxidant inlet temperature then becomes 984 K. Fig. 7b shows the inlet

Table 5
Main dimensions for the 2 kW system dimensioned for operation on hydrogen and for the 2 kW system dimensioned for operation on natural gas

	l_1 (m)	l_2 (m)	l_{syst} (m)	External diameter (m)	l_{ch} @ 0.6 V/cell (m)	Power @ 0.6 V/cell
2 kW hydrogen	0.7	1.1	0.97	0.256	1.65	2.3 kW
2 kW natural gas	1.4	1.8	1.67	0.256	3.77	2.3 kW

temperatures for this case for a range of electrical power output levels. In Table 5 the characteristic dimensions of the 2 kW systems are listed.

4. Conclusions

It has been demonstrated that the system described here can rely on free convection to transfer air and spent gas through the system, while obtaining the required process temperatures for SOFC operation. It has also become clear that if natural gas is used, which has to be mixed with a large amount of water vapour, the application range for these system is limited to about 2 kW. The system described requires a total length of over 5 m, including the chimney; the system itself is 1.7 m long. Undoubtedly in practice the length of the system can be reduced. For instance, the heat exchangers can make multiple passes, thereby reducing the overall length. Also, in the model, the effect of heat transfer by radiation has been ignored. Radiation will increase the effective heat transfer coefficients, thus reducing the required length for the heat exchangers. This in turn reduces the flow friction of the system, which leads to a shorter chimney. It has also been assumed that the process gases have to remove all process heat (adiabatic operation). In practice, process heat will also be transferred through conduction and convection to the environment. Thus, a lower gas flow is required than for adiabatic operation, an effect which again reduces the system length.

References

[1] H.H. Möbius, B. Rohland, US patent 3,377,203, 1968.
[2] R.J. Boersma, N.M. Sammes, Y. Zhang, J. Aust. Ceram. Soc. 34 (1998) 242.
[3] K. Kendall, M. Prica, in: U. Bossel (Ed.), 1st European Solid Oxide Fuel Cell Forum, Lucerne, 1994, p. 163.
[4] R.J. Boersma, N.M. Sammes, C.J. Fee, Solid State Ionics, 1999, in print.
[5] R.J. Boersma, N.M. Sammes, C. Fee, in: S.C. Singhal (Ed.), Proc. of the 6th SOFC Conference, Honolulu, Hawaii, 1999, in print.
[6] K. Stephan, Chem.-Ing.-Tech. 34 (1962) 207.
[7] R. Byron Bird, W.E. Stewart, E.N. Lightfoot, Physical Transport Phenomena, 1960.